Airborne Measurements of Optical Properties of Tropospheric Aerosols over an Urban Area

By Masayuki Tanaka, Tadahiro Hayasaka and Teruyuki Nakajima
Upper Atmosphere and Space Research Laboratory, Tohoku University,
Sendai 980, Japan

(Manuscript received 3 October 1989, in revised form 9 March 1990)

Journal of the Meteorological Society of Japan
Vol. 68, No. 3
Meteorological Society of Japan

Airborne Measurements of Optical Properties of Tropospheric Aerosols over an Urban Area

By Masayuki Tanaka, Tadahiro Hayasaka and Teruyuki Nakajima

Upper Atmosphere and Space Research Laboratory, Tohoku University, Sendai 980, Japan
(Manuscript received 3 October 1989, in revised form 9 March 1990)

Abstract

Aircraft measurements of aerosol sizes, intensities of direct-solar and circumsolar (aureole) radiations, and upward and downward fluxes of solar radiation were carried out over Nagoya, a typical urban area in Japan, using an optical particle counter, an aureolemeter and spectral pyranometers, respectively. Vertical profiles of optical thicknesses and volume spectra of aerosols have been successfully retrieved by inverting measured aureole intensities. The obtained values have been utilized to estimate the absorption indices of aerosols from the downward flux measurements. The results are summarized as follows:

1) The concentration and the vertical stratification of tropospheric aerosols vary considerably day by day.

2) Bimodal volume spectra of aerosols with radii smaller and larger than $r \sim 0.5\ \mu$m generally prevail in the troposphere. The former is more predominant than the latter in the haze layer, and viceversa above that layer.

3) Estimated values of the imaginary index of refraction of tropospheric columnar aerosols are within the range of 0.005~0.014 in the visible region and 0.008~0.020 in the near infrared region. Corresponding values for the haze layer are slightly larger, *i.e.* 0.007~0.018 and 0.011~0.028 in the visible and near infrared regions, respectively.

1. Introduction

Airborne solar radiation measurements have been attempted by several investigators as a means of inferring the vertical stratification and optical properties of aerosols. Among them, Deluisi *et al.* (1976a, b) have made exploratory field experiments involving aircraft measurements of both aerosol concentrations and solar radiation fluxes and also ground-based lidar soundings. Size distributions and vertical distributions of aerosols, and the imaginary part of their complex refractive indices have been determined in a way consistent with radiative transfer theory and with direct observations of absorption in a volume of atmosphere. Values of around 0.01 were obtained for the imaginary index of refraction of aerosols in an arid desert region near Blythe, California and in a semi-arid agricultural region near Big Spring, Texas, comparing favorably with the results of other investigators. Kondratyev *et al.* (1981) have also made aircraft radiative flux measurements at several altitudes in the Saharan dust layer. They found that the size distribution of aerosols could be represented by quadramodal combinations of gamma functions and that, with sufficient variation of the quadramodal size distributions, it was possible to bring calculated and measured radiative fluxes across the entire wavelength region of 0.4~0.9 μm into agreement. Twitty *et al.* (1976) and Nakajima *et al.* (1986) have attempted airborne measurements of the aureole intensity, and retrieved successfully the size distribution and vertical profile of the optical thickness of aerosols. Most of these aircraft measurements have been made in rural regions with fairly homogeneous surface conditions such as deserts, agricultural lands and open waters, and those in urban area are very limited and unsatisfactory (Laulainen *et al.*, 1978; Kobayashi and Yano, 1982). In fact, accurate determinations of vertical profiles of the optical thickness and size distribution of aerosols from airborne radiation measurements are still very difficult and, thus, the agreements among the results obtained by various techniques are not always satisfactory. This is because the concentration of aerosols generally decreases rapidly with altitude, especially above the haze layer, and the accuracy required in radiation measurements is much higher for aircraft measurements than for ground-based measurements.

In the present study, we developed a spectral scanning radiometer (or aureolemeter) to measure

both the direct-solar and circumsolar radiations with a reasonable precision. Spectral pyranometers were also developed for the measurements of spectral fluxes of upward and downward solar radiations. Airborne solar radiation measurements were carried out with these instruments over an urban area around Nagoya, one of the "millions-cities" in Japan. Vertical stratifications of the aerosol optical thickness and volume size spectra of columnar aerosols were successfully retrieved from the aureolemeter measurements. The imaginary (or absorption) indices of refraction of aerosols were estimated from the spectral flux measurements for several wavelengths from visible to near infrared, by utilizing the aerosol volume spectra thus obtained.

2. Details of instrumentation and observation

A CESSNA 206 aircraft was equipped with the aureolemeter, upward and downward looking spectral pyranometers and an optical particle counter. These instruments were mounted on a rigid aluminum rack carefully designed to absorb the vibration of the aircraft body. The aircraft was also equipped with a video camera to monitor the ground surface conditions. All the measured data, together with the ambient pressure and temperature and the pitching and rolling angles of the aircraft, were recorded by a computer-controlled data logging system.

Details of the aureolemeter have been described in Nakajima *et al.* (1986), so a brief description will be given here. This instrument is a spectral scanning radiometer with a light detector of a PIN silicon photo-diode and seven interference filters of wavelengths of 332, 368, 500, 675, 777, 862 and 937 nm. The respective halfwidths of the interference filters were 5, 9, 2, 3, 2, 5 and 5 nm. The aureolemeter with a solid angle of 0.001524 steradian could aim at any direction by a zenith/azimuth DC servo motor system. The position of the sun was continuously monitored by a silicon position-sensitive detector. Both of the direct-solar and circumosolar radiations were measured by using a linear current/voltage converter with a wide dynamic range of 10^5. The entire system was compactly assembled in a spherical aluminum container of 260 mm in diameter and mounted in the rear space of the aircraft. Such a size restriction for our instrument limited the measureable scattering angles (*i.e.* the minimum measurable angle from the sun) to about 5°, due to the length of the sunshade hood. A newly developed method (Tanaka *et al.*, 1986) was applied to calibrate this instrument.

Two spectral pyranometers have been developed for aircraft measurements of upward and downward fluxes of solar radiation. Each of these instruments was equipped with a silicon photo-diode light detector and four interference filters with central wavelengths of 500, 675, 776 and 862 nm which are very close to the corresponding filters of the aureolemter. The incident radiation was collected by a quartz diffuser and was guided to the filter-detector system through a quartz rod of 30 cm in length and 1 cm in diameter to attain large utilization efficiency of light passing through the diffuser. Each instrument protruded from the aircraft body to avoid contaminations due to reflected radiation. Calibration constants of the pyranometers (*i.e.* responses of the pyranometers to the extraterrestrial solar fluxes) were determined by an occultation method using a well calibrated sunphotometer of Tanaka *et al.* (1986) as a standard. A deviation of the incident angle dependence of the pyranometer response from the ideal cosine law was corrected by the aid of transfer theory as shown in the Appendix. A dependence of the pyranometer response on the azimuth angle was found to be so small that no correction was made for it. The temperature correction for the pyranometer response was made by monitoring the ambient temperature around the filter-detector system, using the calibration curve established with an artificial light source in a low temperature room.

The optical particle counter (RION KC-01) was used to measure cumulative particle numbers for radii of $r>0.15$, $r>0.25$, $r>0.5$, $r>1.0$, and $r>2.5$ μm, separately. The air sample of 270 ml was collected for each sampling interval of 45 sec through an intake tube of 1cm in diameter and 100 cm in length and an isokinetic tube with a diameter of 10 cm and a length of 100 cm.

Measurements were carried out over Nagoya on JAN. 14, 1984, NOV. 7 and 8, 1984 and OCT. 9, 1985, under cloudless conditions. Nagoya is located to the north coast of Ise Bay, holding a large industrial area. Ground surface conditions are asphalt roads or concrete buildings in the central area of the city, whereas most of the area in the suburbs is agricultural lands in fallow, covered by withered grass or naked soil, in these seasons from autumn to winter (Fig. 1). The aircraft ascended and descended two times during each measurement; two or three hours were needed in all.

3. Vertical profiles of optical thickness and size distribution of aerosols

The ratios of the observed aureole intensities to the direct-solar intensities at wavelengths of 368, 500, 675, 777 and 862 nm were analyzed with an algorithm developed by Nakajima *et al.* (1983, 1986) to retrieve both the optical thickness and the size distribution of aerosols. The algorithm involves iterations of two steps, *i.e.* the step of subtraction of multiply scattered radiation from measured data by means of a radiative transfer code of calculating the solar aureole and the step of inverting the size distribution (volume spectrum) of aerosols from the forward part of the aerosol phase function. In this

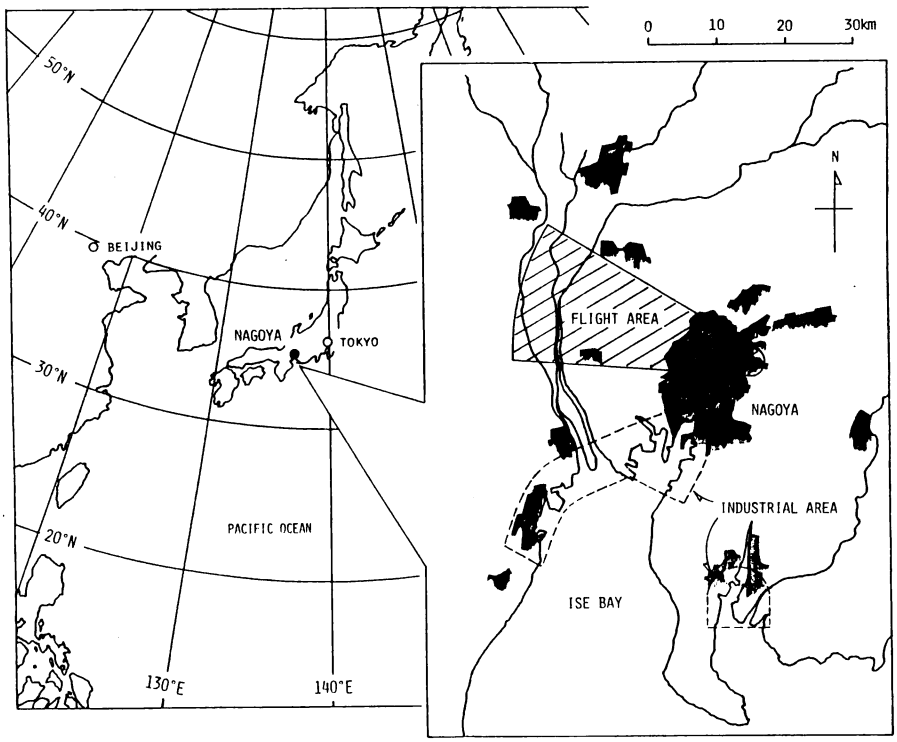

Fig. 1. Location of Nagoya city and its surrounding area. Finely hatched parts indicate dense urban area, and roughly hatched ones the flight area.

algorithm, we used Mie theory for the calculation of the aerosol phase function, assuming for convenience of mathematical treatment that the phase function of aerosols is expressed by that of optically equivalent spherical particles. Although aerosols are not spherical particles in most cases, differences in the forward part of the phase function are small between spherical and nonspherical particles, especially for small particles with x $(=2\pi r/\lambda)$ <5 (Asano and Sato, 1980; Pllack and Cuzzi, 1980). The complex refractive index of aerosols was assumed to be known for this calculation. Many investigators have attempted to estimate this quantity, and found that the real and imaginary in dices of refraction were typically within the range of 1.45~1.55 and 0.005~0.02, respectively, for the tropospheric aerosols (*e.g.* Grams *et al.*, 1974; Patterson *et al.*, 1977; Reagan *et al.*, 1980; Tanaka *et al.*, 1983). The value of refractive index, $\tilde{m}$ = 1.50–0.01i was assumed in this study. The error in the retrieved total optical thickness (the optical thickness for extinction) due to the uncertainty of assumed refractive index was examined by analyzing the data with several different values, *i.e.* $\tilde{m}$ = 1.45–0.01i, 1.50–0.0i, 1.50–0.3i, and 1.55–0.01i. The results for NOV. 7, 1984 are shown in Table 1 for λ = 500 nm. Also shown in the Table are values of the optical thickness for scattering τ_{sca} $(= \omega_o \tau$, ω_o being the albedo for single scattering). The optical thickness for extinction depends on both real and imaginary parts of the refractaive index, while that for scattering depends mainly on the real part. Uncertainties of our retrieval due to the uncertainty of the refractive index are within ±10 % or a little more for τ, and ±5 % or a little more for τ_{sca}. These uncertainties could be eliminated, in principle, by determining the total optical thickness directly from spectral extinction measurements. Such a direct method is, however, of no practical use because the calibration constants of the aureolemeter (or sunphotometer) have to be established with an extremely high accuracy; an accuracy of ±0.3 % is required to determine the optical thickness of 0.03, a typical value of τ at λ = 500 nm in the middle troposphere, with an accuracy of ±10 %.

Vertical profiles of the optical thickness of aerosols from the top of the atmosphere to the respective flight levels are shown in Fig. 2 for λ = 500 nm. Open circles and dotted lines are the values of the optical thickness retrieved from aureole measurements and particle counter measurements, respectively. Fairly small scatterings of the aureolemeter results suggest that both of our radiation measurements and retrievals are reliable; the rms errors are almost comparable with those arising from the uncertainty of the complex refractive index. Since the aircraft ascended and descended two times in each measurement, the results in Fig. 2 suggest that the concentration of aerosols in the lower troposphere is fairly constant within a few hours in the same day, though it changes considerably day by day. Typical haze layers were observed with the eye below 900

Table 1. Aerosol optical thicknesses for extinction (τ) and scattering (τ_{sca}) retrieved from the aureolemeter measurements on NOV. 7, 1984, for $\lambda = 500$ nm and various values of the refractive index.

PRESSURE	1.45–0.01i		1.50–0.0i		1.50–0.01i		1.50–0.03i		1.55–0.01i	
(mb)	τ	τ.sca	τ	τ.sca	τ	τ.sca	τ	τ.sca	τ	τ.sca
1019	0.3013	0.2682	0.2887	0.2887	0.3257	0.2874	0.3814	0.2904	0.3496	0.3073
958	0.1902	0.1571	0.1581	0.1581	0.1849	0.1588	0.2066	0.1561	0.1941	0.1685
934	0.1442	0.1235	0.1242	0.1242	0.1531	0.1309	0.1781	0.1305	0.1622	0.1395
924	0.0825	0.0727	0.0811	0.0811	0.0913	0.0795	0.1086	0.0793	0.0967	0.0850
905	0.0616	0.0510	0.0503	0.0503	0.0619	0.0521	0.0690	0.0505	0.0656	0.0552
862	0.0532	0.0451	0.0478	0.0478	0.0581	0.0488	0.0627	0.0463	0.0625	0.0529
734	0.0421	0.0357	0.0353	0.0353	0.0451	0.0388	0.0521	0.0370	0.0431	0.0377
671	0.0343	0.0300	0.0316	0.0316	0.0369	0.0322	0.0432	0.0319	0.0393	0.0343
642	0.0334	0.0298	0.0320	0.0320	0.0360	0.0320	0.0403	0.0313	0.0389	0.0349
574	0.0271	0.0234	0.0252	0.0252	0.0291	0.0253	0.0359	0.0251	0.0307	0.0268
550	0.0273	0.0236	0.0249	0.0249	0.0293	0.0254	0.0354	0.0251	0.0310	0.0270
468	0.0259	0.0236	0.0243	0.0243	0.0264	0.0238	0.0312	0.0237	0.0280	0.0253

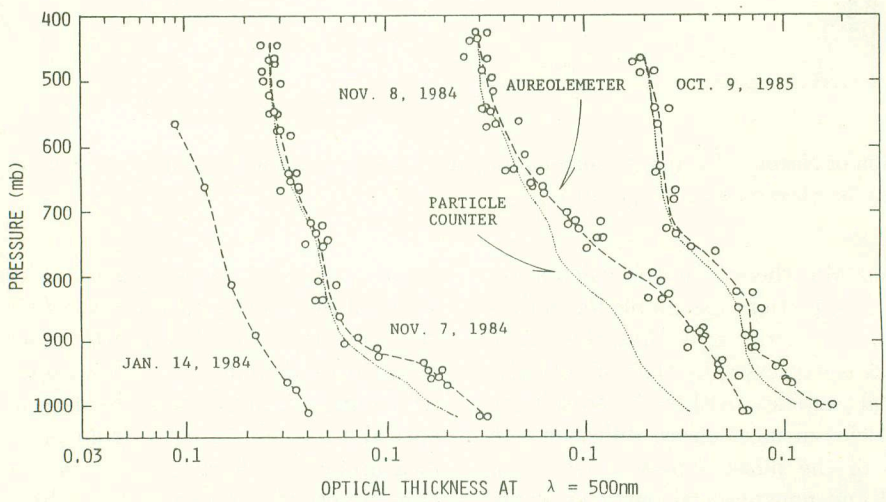

Fig. 2. Vertical profiles of the optical thickness of aerosols at $\lambda = 500$ nm. Open circles and dotted lines show the results obtained from the aureolemeter and the particle counter measurements, respectively.

mb, 800 mb and 880 mb on NOV. 7, NOV. 8, 1984 and OCT. 9, 1985, respectively, in agreement with the results in Fig. 2. The results from the particle counter measurements are systematically underestimated. The discrepancy may partly be attributed to the loss of particles through the intake tube by adsorption of particles or by vaporization of water from hygroscopic substances.

The optical thicknesses of aerosols retrieved from aureolemeter measurements are shown in Fig. 3 as a function of wavelength. The optical thickness of aerosols can be represented, in the first approximation, by Ångström's law (Ångström, 1964), as

$$\tau(\lambda) = \beta\lambda^{-\alpha}, \tag{1}$$

where α is the wavelength parameter and β is the Ångström's turbidity coefficient (optical thickness at the wavelength $\lambda = 1\,\mu$m). It is obvious from the figure that both α and β varied considerably day by day, and from level to level. The values of α range from 0.8 to 1.5 expect for the smaller value at 564 mb on JAN. 14, 1984, comparing favorably with the results of previous investigators. The value of α at the highest flight level on JAN. 14, 1984 may be ascribed to stratospheric aerosols due to the El Chichon eruption. It is also found that the values of β (or optical thicknesses of aerosols) at the maximum flight levels decreased with time, especially in 1984. This phenomenon can be attributed to the decay of stratospheric aerosols originating from the El Chichon eruption, as will be discussed later. The complex refractive index of aerosols we adopted (*i.e.* $\tilde{m} = 1.50$–0.01i) is not suitable for the stratospheric aerosols so that the retrieved optical thicknesses are expected to be overestimated especially at the maximum flight levels. Closed circles in Fig. 3 show the optical thicknesses of aerosols at the maximum flight

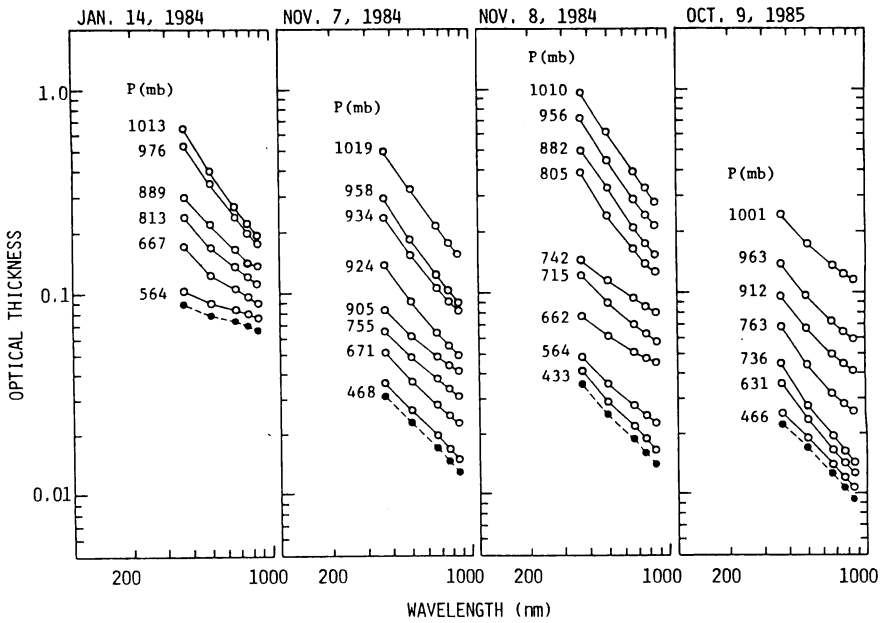

Fig. 3. Optical thicknesses of aerosols versus wavelength at various altitudes. Open and closed circles show the results retrieved with the refractive index of 1.50–0.01i and 1.45–0.0i, respectively.

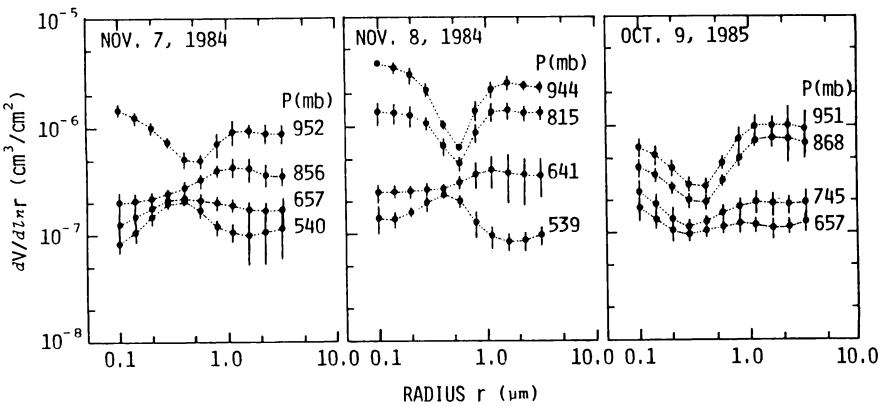

Fig. 4. Volume spectra of columnar aerosols estimated from Aureolemeter measurements at several altitudes on NOV. 7 and 8, 1984 and OCT. 9, 1985.

levels retrieved by assuming $\tilde{m}$ = 1.45–0.0i to fit the refractive index of aerosols to sulfuric acid particles in the stratosphere. The optical thickness for $\tilde{m}$ = 1.45–0.0i are smaller by about 10 % than, but their wavelength dependence is almost similar to the results for $\tilde{m}$ = 1.50–0.01i shown by open circles in the same figure.

Size distributions of aerosols were retrieved from the aureolemeter data with the algorithm outlined before. Since the measured aureole intensities were restricted for scattering angles between 5° and 40°, the retrieved size distributions are reliable only for particle radii around 0.1~3.0 μm; aureole intensities for smaller scattering angles are essential for the retrieval of larger particles (Tanaka *et al.*, 1982; Takamura and Tanaka, 1985; Nakajima *et al.*, 1986). The volume spectra of columnar aerosols retrieved with $\tilde{m}$ = 1.50–0.01i are shown in Fig. 4, averaging several results around the respective indicated levels. The absolute values but not the relative shapes of the volume spectra are influenced by the assumed refractive index, as expected from the results shown in Fig. 3. Typical bimodal spectra prevailed in the lowest layer (or haze layer), while the small particle mode with radii $r < 0.5\,\mu$m disappeared and a rather Junge-like (*i.e.* power law) spectra prevailed above the haze layer. At the uppermost level, on the other hand, the influence of volcanic aerosols due to the El Chichon eruption was clearly detected around the mode radius of 0.4 μm for the results on NOV. 7 and 8, 1984, which almost disappeared on OCT. 9, 1985. Closely similar trends of the influence of the El Chichon eruption were also detected around Japan (Asano *et al.*, 1985; Nakajima *et al.*, 1986; Tanaka *et al.*, 1987).

The size distributions retrieved from the aure-

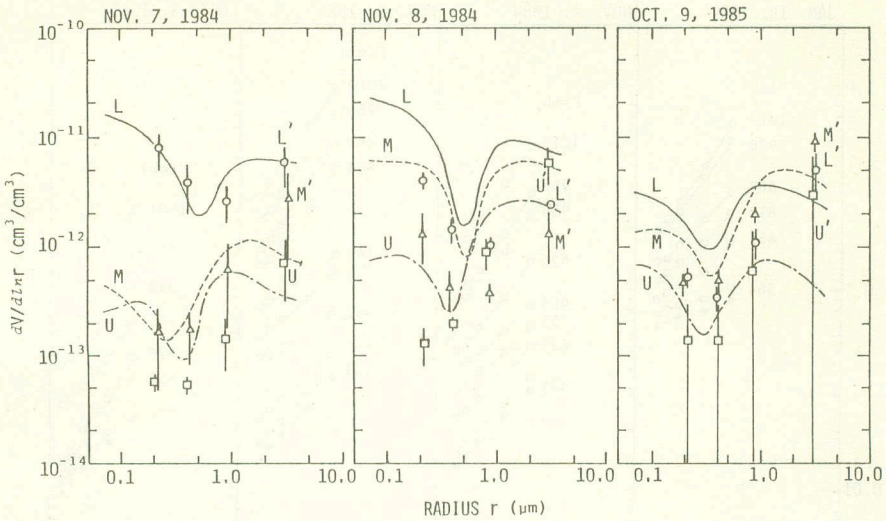

Fig. 5. Volume spectra of aerosols for various layers of the troposphere. Solid (L), broken (M) and dashed-dotted (U) lines show the results from aureolemeter measurements, and circles (L′), triangles (M′) and squares (U′) with error bars those from particle counter measurements. Pressure levels of the respective layers are 856–952 mb (L), 868–968 mb (L′), 657–856 mb (M), 671–856 mb (M′), 540–657 mb (U) and 556–614 mb (U′) for NOV. 7, 815–944 mb (L), 842–938 mb (L′), 641–815 mb (M), 687–815 mb (M′), 539–641 mb (U) and 536 641 mb (U′) for NOV. 8, and 868–951 mb (L), 869–940 mb (L′), 745–868 mb (M), 724–833 mb (M′), 657–745 mb (U) and 656–749 mb (U′) for OCT. 9.

olemeter data are compared with those obtained directly from particle counter measurements, as shown in Fig. 5. Solid, broken and dash-dotted lines show the volume spectra of aerosols in lower (L), middle (M) and upper (U) levels, respectively, which are obtained from aureolemeter measurements as differences of columnar volume spectra between the adjacent two levels shown in Fig. 4. Open circles, triangles and squares with error bars show the volume spectra obtained from particle counter measurements for lower (L′), middle (M′) and upper (U′) layers, respectively. Since the optical particle counter (RION KC-01) was originally calibrated by polystyrene particles with $\tilde{m} = 1.59–0.0i$, we corrected the results for $\tilde{m} = 1.50–0.01i$. The particle counter results are systematically smaller than the aureolemeter results except for the largest radius, showing more coarse particle rich distributions. Such underestimations of the volume spectra by the optical particle counter may partly be attributed to the loss of particles through the intake tube by adsorption of particles or vaporization of water from hygroscopic substances. As for the coarse particle-rich distributions obtained by the particle counter, an inappropriate correction for the refractive index may be responsible. The refractive index correction is much more sensitive for larger radii than for smaller radii, and the value of the imaginary index of 0.01 may be too large for the coarse mode aerosols predominated by soil derived particles (Grams *et al.*, 1974; Reagan *et al.*, 1980; Deepak and Gerber, 1983).

Bimodal volume spectra of aerosols with radii smaller and larger than $r \sim 0.5\,\mu$m were generally prevailing in the troposphere. The respective modes correspond essentially to the accumulation mode and coarse particle mode of Whitby (1978). The accumulation mode was rather more predominant than the coarse particle mode within the haze layer, and vice versa above that layer. Such a predominance of the coarse particle mode above the haze layer has also been observed in the United States by the impactor measurements (Blifford and Ringer, 1969; Gillette *et al.*, 1978), and in Europe and Japan by the optical particle counter measurements (Fitch and Cress, 1981 and 1983; Kobayashi and Yano, 1982). Shettle and Fenn (1979), on the other hand, have proposed unimodal volume spectra consisting only of an accumulation mode for the "Tropospheric aerosol model" above the mixed layer. This contradiction may be ascribed to the difference in the airmass origin. It is well recognized that the physical separation of the accumulation and coarse particle modes arises because the condensation and coagulation processes produce the former, while the mechanical processes produce mostly the latter (Whitby, 1978). Strong westerlies are prevailing in the middle troposphere over Japan throughout the year except for summer. Trajectory analyses for our measurements showed without exception that the airmasses over desert areas in the central Asia reached Nagoya within 2 or 3 days. The wind-blown dust injected into the atmosphere is, thus, considered to be the significant component of the coarse particles observed above the haze layer. Our recent measurements showed that the coarse par-

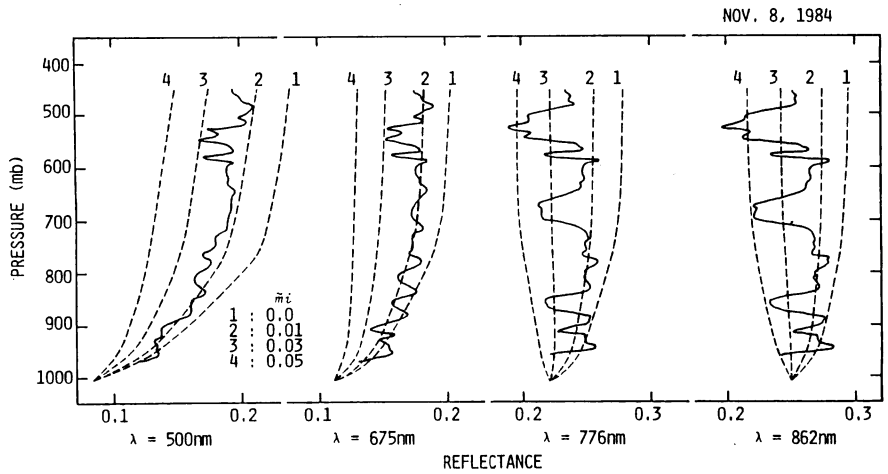

Fig. 6. Vertical profiles of measured (solid lines) and calculated (broken lines) reflectances at $\lambda = 500$, 675, 776 and 862 nm on NOV. 8, 1984. Curves 1, 2, 3 and 4 correspond to $\tilde{m}_i = 0.0$, 0.01, 0.03 and 0.05, respectively.

ticle mode decreased drastically above the mixed layer in the summer season when the Pacific High prevailed over Japan, due to the lack of soil particles supplied from the Asian continent (Hayasaka *et al.*, 1990). The mass loading of the dust particles measured in the present study is of the order of 0.1 ton/km^2 which is about 10 % of the values for the major Yellow Sand (or Kosa) events in the spring season (Iwasaka *et al.*, 1983).

4. Absorption index of aerosols

An orthodox method to estimate the imaginary index of refraction (or absorption index) of aerosols from the net flux convergence is not always applicable to the urban area because the horizontal homogeneity of the surface reflectance is not generally satisfied there. Figure 6 illustrates examples of measured reflectances of the atmosphere-surface system for $\lambda = 500$, 675, 776 and 862 nm comparing with theoretical values for the aerosol absorption indices of $\tilde{m}_i = 0.0$, 0.01, 0.03, and 0.05. The real index of refraction was assumed to be $\tilde{m}_r = 1.50$, and the retrieved values of the optical thickness and the size distribution of aerosols were adopted for this calculation. The fluctuation of the measured reflectance increases with an increase of the wavelength and amounts to about 0.05 at $\lambda = 862$ nm. Such a fluctuation is mainly attributed to different surface conditions for different locations, *i.e.* the maximum values for the far suburbs and the minimum values for the central area of the city. However, even if we sample the data above the same location, their vertical profiles are still different from those calculated for a fixed value of the absorption index. This discrepancy may be ascribed to the change of the effective surface area viewed by the downward-looking pyranometer with altitude; the effective surface area is very narrow at the lowest flight level and expands rapidly with the increase of the flight level. The uncertainty of the upward flux due to this change of the surface albedo brings about a large uncertainty of the net flux convergence, especially for the small convergence values.

We therefore attempted to retrieve the absorption index of aerosols from measured downward fluxes instead of the net flux convergence. The downward flux F at a pressure P can be approximated by

$$F = \frac{F_0}{1 - R\bar{s}}, \tag{2}$$

where F_o is the downward flux at the level P excluding the effect of reflection from the underlying atmosphere-surface system, R is the reflectance of that system which is assumed to be Lambertian, and $\bar{s}$ is the downward reflectance of the overlying atmosphere for isotropic incidence. When R changes by ΔR, the downward flux changes by ΔF, as

$$\Delta F = \frac{F_0}{1 - (R + \Delta R)\bar{s}} - \frac{F_0}{1 - R\bar{s}} \sim F_0 \Delta R \bar{s}. \tag{3}$$

Since the value of $\bar{s}$ is typically 0.2 or less, the error of 0.05 in the reflectance affects F values only by 0.01 at most. Figure 7 shows an example of the measured downward flux (solid line) compared with calculated values for $\tilde{m} = 0.0$, 0.01, 0.03 and 0.05 (broken lines). Both fluxes in Fig. 7 are normalized by the horizontal flux of the incident solar radiation at the top of the atmosphere. The dependence of the calculated downward flux on the aerosol absorption index is much larger than the fluctuation of measured values and, thus, the optimum values of the absorption index can be inferred from the least-squares fitting between measured and calculated profiles of the downward flux. The absorption indices thus obtained are shown in Table 2. The

radiative transfer calculations have been performed by a matrix adding method based on the optical thicknesses for scattering and the size distribution of aerosols retrieved from the aureolemeter measurements, and on the measured surface albedos. The analyses are performed for both the total and haze layers on NOV. 7 and 8, 1984. In the analyses for the haze layer, the flux differences between the top of the haze layer and the respective levels within the haze layer were compared with theoretical results for various of $\tilde{m}_i$. The absorption indices of tropospheric aerosols (total layer) are within the range of 0.005~0.014 in the visible region and 0.008~0.020 in the near infrared region. Corresponding values for the haze layer are slightly larger, *i.e.* 0.007~0.018 and 0.011~0.028 in the visible and near infrared regions, respectively. These values are much smaller than the absorption indices of urban aerosols compiled by Deepak and Gerber (1983), but are closely similar to the results of polar nephelometer measurements in Sendai, Japan (Tanaka *et al.*, 1983) and the results for rural, remote or soil derived aerosols of previous investigators (Deepak and Gerber, 1983). The wavelength dependence of the absorption index is consistent with that of water soluble particles consisting of the main part of the tropospheric aerosols (Shettle and Fenn, 1979; Deepak and Gerber, 1983). The values in parentheses in Table 2 show the absorption indices retrieved by adopting the power law volume spectra estimated from Eq. (1). The retrieved absorption indices are affected by a factor of two by this alternation; it is important to determine the aerosol size distribution as accurate as possible for and accurate determination of the absorption index.

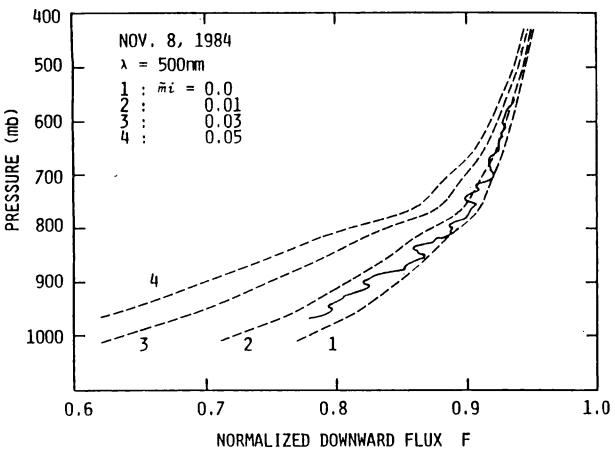

Fig. 7. Vertical profiles of measured (solid line) and calculated (broken lines) downward fluxes at $\lambda = 500$ nm on NOV. 8, 1984.

5. Summary

We investigated optical properties of tropospheric aerosols in an urban area by airborne solar radiation measurements with the aureolemeter and spectral pyranometers. Optical thicknesses and volume size distributions of columnar aerosols above each altitude in the troposphere were retrieved by inverting the solar aureole intensities. The size distributions retrieved from the aureolemeter measurements were compared with those obtained by the particle counter in the middle, lower and lowermost tropospheres, respectively. The absorption indices of tropospheric aerosols were estimated from downward flux measurements by the spectral pyranometers. Results of the present investigation are summarized as follows:

1) The concentration of aerosols in the troposphere changes considerably day by day, but is fairly constant within a few hours for the same day.

2) Bimodal volume spectra of aerosols with radii smaller and larger than $r \sim 0.5\,\mu$m, *i.e.* the accumulation and coarse particle modes, are generally prevailing in the troposphere (in and above the haze layer). The accumulation mode is rather more pre-

Table 2. Absorption indices of aerosols in the total column (TOTAL) and the haze layer (HAZE) at $\lambda = 500$, 675, 776 and 862 nm. Values in the parentheses are the absorption indices retrieved by adopting the power-law size distribution.

DATE			LAYER	WAVELENGTH (nm) 500	675	776	862
JAN.	14,	1984	TOTAL	(0.010±0.003)	(0.009±0.003)	(0.010±0.002)	(0.010±0.002)
NOV.	7,	1984	TOTAL	0.013±0.001	0.014±0.001	0.020±0.001	0.018±0.002
				(0.017±0.001)	(0.020±0.001)	(0.030±0.001)	(0.027±0.002)
			HAZE	0.016±0.001	0.018±0.001	0.024±0.001	0.028±0.002
NOV.	8,	1984	TOTAL	0.007±0.002	0.005±0.002	0.009±0.002	0.009±0.003
				(0.007±0.001)	(0.006±0.002)	(0.011±0.002)	(0.012±0.003)
			HAZE	0.007±0.002	0.008±0.003	0.011±0.002	0.012±0.003
OCT.	9,	1985	TOTAL	0.005±0.002	0.006±0.002	0.011±0.002	0.008±0.002
				(0.011±0.002)	(0.013±0.002)	(0.022±0.002)	(0.016±0.002)

dominant than the coarse particle mode in the haze layer, and viceversa above that layer. The wind blown dust injected from desert areas in the central Asia is considered as the origin of the coarse particle mode prevailing above the haze layer.

3) Absorption indices of tropospheric columnar aerosols are within the range of 0.005~0.014 in the visible region and 0.008~0.020 in the near infrared region. Slightly larger values of 0.007~0.018 and 0.011~0.028 are retrieved for the haze layer in the visible and near infrared regions, respectively. These values of the absorption index are much smaller than those of typical urban aerosols, and almost comparable to the absorption indices of rural aerosols. Such a result may be attributed partly to the fact that the occurrence of dense urban aerosols is rather restricted in the surface boundary layer under stable meteorological conditions.

Acknowledgments

The authors are grateful to Y. Nakanishi for his technical assistance. Personnel and the flight facility of Nakanihon Air Service Co. are acknowledged for their efforts during the experimental periods. This research was partly supported by Funds for the Middle Atmosphere Program (MAP) from the Ministry of Education, Science and Culture, Japan.

Appendix

Correction of Flux Data

In order to correct the effect of non-ideal angular response of the pyranometer on the downward flux, we use the following relation:

$$F^{\downarrow} = (F^{\downarrow\prime} - \mu_0' D_0 K(\mu_0'))/\tilde{K}^{\downarrow} + D_0\mu_0, \qquad \text{(A1)}$$

where $F^{\downarrow}$ is the corrected downward flux, $F^{\downarrow\prime}$ is the measured downward flux, D_0 is the intensity of direct solar radiation measured by the aureolemeter, μ_0 is the cosine of the solar zenith angle, μ_0' is the apparent value of μ_0 due to pitching and rolling of the aircraft, $K(\mu)$ is the angular response of the pyranometer at $\theta = \cos^{-1}\mu$, and $\tilde{K}^{\downarrow}$ is the correction factor. The value of K can be estimated from the definition, as

$$\tilde{K}^{\downarrow} = 2\pi \int_0^1 I(\mu)K(\mu)\mu d\mu \Big/ 2\pi \int_0^1 I(\mu)\mu d\mu, \qquad \text{(A2)}$$

where $I(\mu)$ is the azimuthally averaged intensity of diffuse sky radiation. The same radiative transfer code as mentioned in the text was used to calculate the sky radiance distribution, based on the optical thickness for scattering and the size distribution of aerosols retrieved from the aureolemeter measurements.

As for the correction of the upward flux, we assumed that the intensity of diffuse radiation is isotropic, *i.e.* $I(\mu) = I_0$. The corrected value of the upward flux, $F^{\uparrow}$ is then given by

$$F^{\uparrow} = F^{\uparrow\prime} / \tilde{K}^{\uparrow}, \qquad \text{(A3)}$$

where $F^{\uparrow\prime}$ is the measured upward flux, and $\tilde{K}^{\uparrow}$ is the correction factor given by

$$\tilde{K}^{\uparrow} = 2\pi \int_0^1 I_0 K(\mu)\mu d\mu \Big/ 2\pi \int_0^1 I_0\mu d\mu = 2\int_0^1 K(\mu)\mu d\mu. \qquad \text{(A4)}$$

References

Ångström, A., 1964: The parameters of atmospheric turbidity. *Tellus*, **16**, 64–75.

Asano, S. and M. Sato, 1980: Light scattering by randomly oriented spheroidal particles. *Appl. Opt.*, **19**, 962–974.

Asano, M. Sekine, M. Kobayashi and K. Murai, 1985: Atmospheric turbidity and aerosol size distribution in winter at Tsukuba: Effects of the El Chichon. *J. Meteor. Soc. Japan*, **63**, 453–463.

Blifford, I.H. Jr. and L.D. Ringer, 1969: The size and number distribution of aerosols in the continental troposphere. *J. Atmos. Sci.*, **26**, 716–726.

Deepak, A. and H.E. Gerber, 1983: Report of the experts meeting on aerosols and their climatic effect. WMO/WCP-55, 107pp.

Deluisi, J.J., P.M. Furukawa, D.A. Gillette, B.G. Scuster, R.J. Charlson, W.M. Porch, R.W. Fegley, B.M. Herman, R.A. Rabinoff, J.T. Twitty and J.A. Weinman, 1976a: Results of a comprehensive atmospheric aerosol-radiation experiment in the southwestern United States. Part I: Size distribution, extinction optical depth and vertical profiles of aerosols suspended in the atmosphere. *J. Appl. Meteor.*, **15**, 441–454.

Deluisi, J.J., P.M. Furukawa, D.A. Gillette, B.G. Scuster, R.J. Charlson, W.M. Porch, R.W. Fegley, B.M. Herman, R.A. Rabinoff, J.T. Twitty and J.A. Weinman, 1976b: Results of a comprehensive atmospheric aerosol-radiation experiment in the southwestern United States. Part II: Radiation flux measurements and theoretical interpretation. *J. Appl. Meteor.*, **15**, 455–463.

Fitch, B.W. and T.S. Cress, 1981: Measurements of aerosol size distributions in the lower troposphere over Northern Europe. *J. Appl. Meteor.*, **20**, 1119–1128.

Fitch, B.W. and T.S. Cress, 1983: Spatial and temporal variation of tropospheric aerosol volume distribution. *J. Climate Appl. Meteor.*, **22**, 1262–1269.

Gillette, D.A., R.N. Clayton, T.K. Mayeda, M.L. Jackson and K. Sridhar, 1978: Tropospheric aerosols from some major dust storms of the southwestern United States. *J. Appl. Meteor.*, **17**, 832–845.

Grams, G.W., I.H. Blifford, Jr., D.A. Gillette and P.B. Russell, 1974: Complex index of refraction of airborne soil particles. *J. Appl. Meteor.*, **13**, 459–471.

Hänel, G., 1976: The properties of atmospheric aerosol particles as functions of the relative humidity at thermodynamic equilibrium with the surrounding moist air. *Adv. Geophys.*, **19**, 73–188.

Hayasaka, T., M. Tanaka and T. Nakajima, 1990: The coarse particle aerosols in the free troposphere around Japan. (submitted to *J. Geophys. Res.*)

Iwasaka, Y., H. Minoura and K. Nagaya, 1983: The transport and spacial scale of Asian dust storm clouds: A case study of the dust storm event of April 1979. *Tellus*, **35B**, 189–196.

Kobayashi, T. and N. Yano, 1982: Relation between observed aerosol optical thickness and calculated values from size distribution measurements. *J. Meteor. Soc. Japan*, **60**, 1249–1258.

Kondratyev, K. Ya., R.M. Welch, S.K. Cox, V.S. Grishechkin, V.A., Ivanov and O.B. Vasilyev, 1981: Determination of vertical profiles of aerosol size spectra from aircraft radiation flux measurements 1. Retrieval of spherical particle size distribution. *J. Geophys. Res.*, **86**, 9783–9793.

Laulainen, N.S., A.J. Alkezweeny and J.M. Thorp, 1978: Simultaneous aerosol size distribution and turbidity measurements over St. Louis during METROMEX 1975. *J. Appl. Meteor.*, **17**, 615–626.

Nakajima, T., M. Tanaka and T. Yamauchi, 1983: Retrieval of the optical properties of aerosols form aureole and extinction data. *Appl. Opt.*, **22**, 2951–2959.

Nakajima, T., M. Tanaka, T. Hayasaka, Y. Miyake, Y. Nakanishi and T. Sasamoto, 1986: Airborne measurements of the optical stratification of aerosols in turbid atmospheres. *Appl. Opt.*, **25**, 4374–4381.

Patterson, E.M., D.A. Gillette and B.H. Stockton, 1977: Complex index of refraction between 300 and 700 nm for Saharan aerosols. *J. Geophys. Res.*, **82**, 3153–3160.

Pollack, J.B. and J.N. Cuzzi, 1980: Scattering by nonspherical particles of size comparable to a wavelength: A new semi-empirical theory and its application to tropospheric aerosols. *J. Atmos. Sci.*, **37**, 868–881.

Reagan, J.A., D.A. Byrne, M.D. King, J.D. Spinhirne and B.M. Herman, 1980: Determination of the complex refractive index and size distribution of atmospheric particulate from bistatic-monostatic lidar and solar radiometer measurements. *J. Geophys. Res.*, **85**, 1591–1599.

Shettle, E.P. and R.W. Fenn, 1979: *Models for the aerosols of the lower atmosphere and the effects of humidity variations on their optical properties.* Air Force Geophysics Laboratory, Rep. AFGL-TR-79-0214, 94pp.

Takamura, T. and M. Tanaka, 1985: Some uncertainties in optical properties of aerosols estimated from light scattering measurements. *J. Meteor. Soc. Japan*, **63**, 969–974.

Tanaka, M., T. Nakajima and T. Takamura, 1982: Simultaneous determination of complex refractive index and size distribution of airborne and water-suspended particles from light scattering measurements. *J. Meteor. Soc. Japan*, **60**, 1259–1272.

Tanaka, M., T. Takamura and T. Nakajima, 1983: Refractive index and size distribution of aerosols as estimated from light scattering measurements. *J. Climate Appl. Meteor.*, **22**, 1253–1261.

Tanaka, M., T. Nakajima and M. Shiobara, 1986: Calibration of a sunphotometer by simultaneous measurements of direct-solar and circumsolar radiations. *Appl. Opt.*, **25**, 1170–1176.

Tanaka, M., T. Nakajima, M. Shiobara and T. Hayasaka, 1987: Atmospheric turbidity monitoring by use of a scanning radiometer. Proc. Beijing International Radiation Symposium 1986, 589–595.

Twitty. J.T., R.J. Parent, J.A. Weinman and E.W. Eloranta, 1976: Aerosol size distributions: remote determination from airborne measurements of the solar aureole. *Appl. Opt.*, **15**, 980–989.

Whitby, K.T., 1978: The physical characteristics of sulfur aerosols. *Atmos. Environ.*, **12**, 135–159.

都市域における対流圏エアロゾルの光学的性質の航空機観測

田中正之・早坂忠裕・中島映至

（東北大学理学部附属超高層物理学研究施設）

典型的な都市域の一つである名古屋の上空で、オプティカル・エアロゾル・カウンター、オーリオールメータ、および波長別水平面日射計を用いた航空機観測を実施し、エアロゾルの粒径分布、直達・周辺太陽光強度、および上向き・下向きの水平面日射量を測定した。得られた太陽周辺光強度のインバージョンにより様々な高度におけるエアロゾルの光学的厚さと体積–粒径分布を得、また、それらの結果と波長別の水平面日射量からエアロゾルの吸収係数（複素屈折率の虚数部）の値を見積った。得られた結果は以下の通りである。

1) 対流圏エアロゾルの濃度、成層状態は日によって激しく変化する。

2) エアロゾルの粒径分布は半径 0.5 μm 付近に極小値を持つ二山型をしており、混合層内では小粒子モー

ドが、また、混合層の上では大粒子モードが卓越する傾向が見られる。

3) 見積られた全気柱平均のエアロゾルの複素屈折率の虚数部の値は、可視域で 0.005~0.014 の範囲に、近赤外域で 0.008~0.020 の範囲にあり、波長と共に増加する傾向にある。混合層内での対応する値は可視域で 0.007~0.018 の範囲に、近赤外域で 0.011~0.028 の範囲にあり、全気柱の平均値より若干大きい。